

Innovative power sharing and secondary controls for meshed microgrids

Youssef Amine Ait Ben Hassi¹, Youssef Hennane^{1,2}, Abdelmajid Berdai¹

¹Laboratory of Energy and Electrical Systems, Ecole Nationale Supérieure d'Electricité et de Mécanique (ENSEM), Université Hassan 2 de Casablanca, Casablanca, Morocco

²Laboratory for Energy and Theoretical and Applied Mechanics (LEMETA), Université de Lorraine, Nancy, France

Article Info

Article history:

Received Dec 13, 2023

Revised Aug 23, 2024

Accepted Sep 3, 2024

Keywords:

Distributed generations

Microgrids

Power sharing

Primary control

Secondary control

ABSTRACT

In alternating current (AC) microgrids, the prevalent approach for controlling the power distribution between generators and loads is droop control. This decentralized technique ensures accurate power sharing; however, its utility is restricted by significant drawbacks. Notably, in scenarios involving dissimilar power sources, mismatched impedance lines, or meshed microgrids, conventional droop control fails to ensure effective reactive power sharing among inverters, often leading to notable circulating currents. Hence, the primary objective of this paper is twofold: firstly, to examine limitations inherent to conventional droop control; secondly, to introduce a robust power-sharing methodology for AC microgrids. This novel approach is specifically designed to achieve consistent sharing of active and reactive power across meshed topology microgrids. The technique considers the presence of distributed power loads and the dynamic nature of the topology. Despite the attainment of satisfactory active and reactive power sharing, deviations in voltage and frequency occasionally manifest. To address this issue, a supplementary control mechanism is proposed as a third phase. This secondary control method focuses on reinstating the microgrid's voltage and frequency to rated values, all while upholding the precision of power sharing. The efficacy of this multi-stage methodology is rigorously validated through simulations using MATLAB/Simulink and practical experimentations.

This is an open access article under the [CC BY-SA](https://creativecommons.org/licenses/by-sa/4.0/) license.



Corresponding Author:

Youssef Amine Ait Ben Hassi

Laboratory of Energy and Electrical Systems, Ecole Nationale Supérieure d'Electricité et de Mécanique,

Université Hassan 2 de Casablanca

19, Rue Tarik Bnou Ziad, Casablanca, Morocco

Email: youssefamine.aitbenhassi@gmail.com

1. INTRODUCTION

Given the recurring energy and environmental crises that have marked recent years, there has been a growing emphasis on elevating the proportion of clean energy within the power system [1]–[3]. Yet, the integration of a substantial share of renewable sources poses a significant challenge to the stability of the electrical grid. In response to this challenge, there has been a notable surge in interest regarding microgrids [4], [5].

A microgrid, essentially a scaled-down version of the larger electrical grid, encompasses various components, such as sources, power electronic devices, alternating current (AC) or direct current (DC) buses, transmission lines, loads, and energy storage. It can function autonomously or in connection with the main grid [6]. The generation sources within a microgrid can be either centralized or distributed across

geographical regions. This distribution serves two primary purposes: firstly, to cater to scattered loads, and secondly, to optimize energy efficiency. This innovative concept offers potential economic benefits and holds promise for addressing various social and environmental objectives [7].

In a broader context, maintaining effective control over microgrid dynamics necessitates the implementation of a three-tiered hierarchical control structure [8], comprising primary, secondary, and tertiary controls [9]. The primary control component is pivotal in establishing and stabilizing both voltage and frequency parameters. It also facilitates equitable power distribution among parallel distributed generators (DGs), proportional to their power ratings. Subsequently, the secondary control mechanism comes into play, rectifying any deviations in voltage and frequency that may arise due to the actions of the primary control [10]. In addition, the tertiary control function regulates power flow between the microgrid and the external power grid at the point of common coupling (PCC) [11]. Among these control layers, the focus of this study is on the primary and secondary control layers governing the behavior of parallel inverters interconnected within a shared AC microgrid.

The primary focus within a microgrid revolves around the implementation of a primary control mechanism that guarantees the effective distribution of both active and reactive power among the DGs units. Currently, the droop control technique stands as the most prevalent approach for achieving this power-sharing objective [12]. What sets droop control apart from other strategies is its autonomy from communication requirements, rendering it a distinct method for power sharing [13]. However, it is widely acknowledged that traditional droop control encounters limitations when applied to microgrids characterized by disparate impedances within their line configurations. In such scenarios, the functionality of traditional droop control ensures only adequate sharing of active power, while precise sharing of reactive power remains a significant challenge. In essence, the precise sharing of reactive power presents a substantial constraint within this particular control strategy.

In response to the limitations inherent in traditional droop control, researchers have endeavored to enhance this approach, aiming to mitigate steady-state errors in reactive power distribution. For instance, in [14], an innovative methodology calculates the converters' supplied power through an indirect process, obviating the need to measure DGs' output current. Consequently, this approach reduces reliance on current sensors. This method has been effectively applied to DC microgrids, yielding power-sharing outcomes comparable to the classical droop control technique. Han *et al.* [15] introduced a hierarchical control scheme for DC microgrids. It successfully achieves proficient current sharing among power sources by employing adaptive corrections to droop coefficients. Furthermore, a secondary control mechanism is proposed to ensure the restoration of voltage levels. Meanwhile, Azim *et al.* [16] suggests a proportional power-sharing control strategy tailored for low-voltage AC microgrids. This technique not only ensures accurate sharing of both active and reactive power but also contributes to overall system stability. A novel adaptive improved droop control strategy for voltage source controllers within mesh topology DC microgrids is presented in [17]. The objective here is two-fold: providing frequency support to the AC grid and enhancing stability in grid-connected mode. Meanwhile, Sellamna *et al.* [18] suggests a method that attains proportional power sharing within an AC mono-PCC microgrid. This method takes into account factors such as varying line impedances, intermittent communication, load fluctuations, and time delays, all while maintaining the precision of power sharing. Furthermore, Pham *et al.* [19] addresses power-sharing accuracy through the reduction of voltage drops and the implementation of a sliding mode controller (SMC). The integration of SMC not only enhances power-sharing accuracy but also contributes to improved system stability. The research documented in [20] introduces a decentralized adaptive droop control technique. In this approach, the microgrid's impedance is computed to enable the fine-tuning of droop coefficients. This innovative method has demonstrated multiple benefits, including a reduction in power losses. However, it is worth noting that this approach demands a thorough knowledge of the microgrid's parameters. He and Li [21] propose an advanced control approach. The innovation lies in the estimation of reactive power through a minor disruption in active power. An integral term is introduced into the droop equations to mitigate sharing discrepancies.

Effective distribution of reactive power among parallel units of DGs in AC microgrids, coupled with an enhancement in system stability, can also be attained through the implementation of the virtual impedance strategy. This technique is explored in [22], where the mismatch in lines' impedances is counterbalanced through the addition of a virtual impedance into the system. Notably, active and reactive powers are decoupled in this process. The virtual impedance, characterized by its adaptability and proportionality to the reactive power, contributes significantly to the achievement of this method's objectives. Similarly, a comparable control methodology is detailed in [23], leading to an improvement in reactive power sharing. However, it is important to highlight that a prerequisite knowledge of the lines' impedances is necessary for this approach to be effective.

These initial control measures inherently induce deviations in the system frequency and voltage from their designated values. Consequently, the subsequent hierarchical layer, known as the secondary control, becomes indispensable. Within this context, Micallef *et al.* [24] presents a centralized secondary control scheme that effectively rectifies voltage and frequency discrepancies. It is noteworthy, however, that this method mandates communication between each controller and the centralized unit. In a similar vein, Simpson-Porco *et al.* [25] accomplishes the objectives of secondary control. Nevertheless, a tradeoff emerges between power sharing and voltage regulation. Secondary control has also been harnessed in [26]–[28] to attain reactive power sharing through the compensation of voltage drops.

The main problem addressed in this paper is ensuring the precise distribution of both active and reactive power among DGs within microgrids. When this balance is not achieved, it can lead to some DGs being overloaded while others are underutilized. Additionally, unequal sharing of reactive power can cause voltage instability, impacting the reliability of the entire microgrid.

That is why, this study delved into the development of novel power-sharing and secondary control methods, specifically considering meshed scenarios and working conditions. In contrast to earlier studies, which did not explicitly address certain meshed scenarios, potentially resulting in inefficiencies when applying earlier methods in such contexts [29], [30]. The paper contributes significant contributions through the proposed control scheme, addressing the following identified gaps in previous research: i) Limited exploration in multi-PCC configurations: prior studies predominantly focused on single PCC bus systems, overlooking the more prevalent and intricate multi-PCC configurations encountered in real-world microgrids; ii) Neglecting the influence of mesh topology networks: meshed networks play a crucial role in influencing power sharing among parallel sources, yet this aspect has often been disregarded in earlier research; iii) Neglecting meshed conditions, load variations, and topological changes: earlier literature inadequately accounted for dynamic conditions, such as load variations and alterations in microgrid topology, essential for the development of effective control schemes; iv) Neglecting the accommodation of unequal and randomly dispersed load: previous methods did not address challenges posed by non-uniform distribution and random fluctuations in load demands within microgrids; v) Limited adaptability to variable microgrid topologies: Proposed techniques in earlier studies may not be well-suited for microgrids with changing configurations, a common scenario in real-world applications; and vi) Ignoring secondary control integration with power-sharing methods in meshed microgrids: despite improvements in power-sharing methods, deviations in frequency and voltage persist below rated levels; Therefore, integrating secondary control with power-sharing strategies becomes imperative to further reduce these deviations and enhance overall system stability.

This study presents an innovative control strategy to address the identified gaps above. We found that the suggested method demonstrates promising results, particularly in meshed scenarios, where it achieves accurate power sharing and successfully restores voltage and frequency without any compromise compared to the previous studies in literature, which may not remain correct under the specific conditions considered in this paper. The subsequent sections outline the structure of this paper: In section 2, the paper delves into the problem posed by the constraints of droop control, highlighting its limitations. Section 3 is dedicated to revealing the novel power-sharing control strategy, and explaining its mechanisms and benefits. The presentation of the new secondary control method takes place in section 4. Simulations and experimental validation are elaborated upon in sections 5 and 6, respectively, showcasing the real-world efficacy of the proposed approach. Section 7 serves as the concluding segment of this research paper, summarizing key findings.

2. CONVENTIONAL DROOP CONTROL

2.1. Droop control principle

In a broader context, a microgrid comprises multiple interconnected inverters operating in parallel. Figure 1 illustrates the block diagram of an AC microgrid. These parallel inverters are all linked to a shared bus known as the PCC via transmission lines. The microgrid's local loads are also connected to this PCC point. The microgrid is versatile and capable of functioning in either an isolated (islanded) state or in connection mode with the power grid. During the connected mode, a bypass switch is engaged, facilitating the exchange of power between the utility grid and the microgrid. The conventional droop control mechanism can be explained by considering a simplified equivalent circuit, as depicted in Figure 1. In essence, employing Thevenin's theorem the resultant current generated by DG_i “i,” where $i \in \mathbb{N}$, can be expressed as depicted in (1).

$$I_i = \frac{U_i \angle \delta_i - U_n \angle \delta_n}{Z_i \angle \theta_i} = \frac{U_i \cos(\delta_i) - U_n + j U_i \sin(\delta_i)}{Z_i \angle \theta_i} \quad (1)$$

Here, U_i and δ_i represent the root mean square (RMS) voltage and phase angle of DG_i respectively. Meanwhile, Z_i and θ_i correspond to the magnitude and phase angle of the feeder impedance associated with DG_i .

Based on (1), active and reactive powers can be expressed as in (2) and (3):

$$P_i = \left(\frac{U_i U_n}{Z_i \angle \theta_i} \cos(\delta_i) - \frac{U_n^2}{Z_i \angle \theta_i} \right) \cos(\theta_i) + \frac{U_i U_n}{Z_i \angle \theta_i} \sin(\delta_i) \cos(\theta_i) \quad (2)$$

$$Q_i = \left(\frac{U_i U_n}{Z_i \angle \theta_i} \cos(\delta_i) - \frac{U_n^2}{Z_i \angle \theta_i} \right) \sin(\theta_i) + \frac{U_i U_n}{Z_i \angle \theta_i} \sin(\delta_i) \sin(\theta_i) \quad (3)$$

Given the assumption that the feeder impedances possess a purely inductive character and that δ_i is of negligible magnitude, The (2) and (3) can be simplified to yield (4) and (5):

$$P_i = \frac{U_i x U_n}{x_i} \delta_i \quad (4)$$

$$Q_i = \frac{U_i x U_n - U_n^2}{x_i} \quad (5)$$

The equation (4) and (5) form the foundational framework for the traditional droop control methodology. Specifically, the equation (4) highlights the ability to manipulate reactive power through modulation of the output voltage magnitude. Meanwhile, the equation (5) demonstrates that control over active power can be achieved by manipulating the droop angle, a parameter intricately tied to the frequency of the system. These interrelationships are seamlessly transformed into the formulations as articulated in (6) and (7).

$$w_i = w_{in} - n_i (P_i - P_n) \quad (6)$$

$$U_i = U_n - m_i (Q_i - Q_n) \quad (7)$$

The parameters w_{in} and w_i represent the nominal and reference frequencies of DG unit “i,” respectively. Similarly, U_n and U_i denote the nominal and reference voltages of DG_i . The coefficients m_i and n_i correspond to the slopes associated with the droop control characteristic.

In steady state, the distribution of active power among DGs remains precise. However, achieving balanced sharing of reactive power proves challenging due to impedance disparities, potentially resulting in circulating currents within the inverters. In such instances, the establishment of equitable reactive power sharing necessitates a scenario where line impedances are inversely proportional to the corresponding load demands. Nonetheless, achieving such a proportionality is not straightforward.

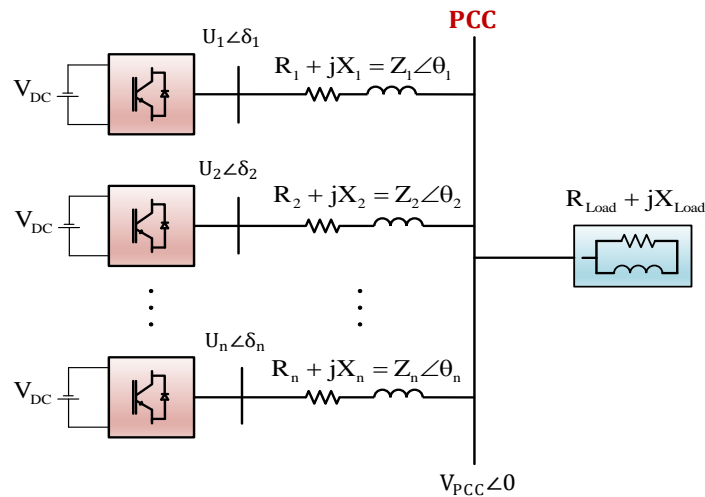


Figure 1. Equivalent model of AC microgrid with n DGs units

2.2. Droop control analysis

In Figure 2, an AC microgrid is considered, Figure 2(a) presents a microgrid with two DGs, transmission lines, and two loads. For the sake of simplicity, DGs power ratings are considered identical and

their voltage droop coefficients are considered equal. As previously highlighted, the chief contributor to imbalanced reactive power sharing arises from the mismatch in feeder impedances. This means that the sharing error is a function of feeders' impedances. The relationship between the sharing error and voltage drops is analyzed in this section.

Microgrid's Q-V equations are expressed in (8) and (9):

$$U_1 = U_n - m(Q_1 - Q_n) \quad (8)$$

$$U_2 = U_n - m(Q_2 - Q_n) \quad (9)$$

The voltage drops between DGs and the node Ni are expressed by (10) and (11):

$$U_1 - U_{N1} = \frac{X_1}{U_n} Q_1 \quad (10)$$

$$U_2 - U_{N2} = \frac{X_2}{U_n} Q_2 \quad (11)$$

where U_{N1} and U_{N2} are Voltage values of nodes N1 and N2, respectively. X_1 and X_2 are feeders' lines inductance, respectively.

Based on (10) and (11), voltage drops due to the interconnection impedance $X_{1,2}$ between DG_1 and DG_2 can be expressed as (12) and (13):

$$U_{N2} - U_{N1} = \frac{X_{1,2}(Q_2 - Q_{L2})}{U_n} = \frac{X_{1,2}(1-A)}{U_n} Q_2 \quad (12)$$

$$\text{Where } A = \frac{QL_2}{Q_2} \quad (13)$$

Using (10) to (13), voltage drops between DGs and node N1 are presented in (14) and (15):

$$U_1 - U_{N1} = \frac{X_1}{U_n} Q_1 = \frac{X'_1}{U_n} Q_1 \quad (14)$$

$$U_2 - U_{N1} = \frac{X_2}{U_n} Q_2 + \frac{X_2(1-A)}{U_n} Q_2 = \frac{X'_2}{U_n} Q_2 \quad (15)$$

$$\text{With } \begin{cases} X'_1 = X_1 \\ X'_2 = X_2 + X_{1,2}(1-A) \end{cases} \quad (16)$$

Thanks to (14) and (15), the considered microgrid can be simplified as shown in Figure 2(b). In this equivalent structure, the PCC bus is confused with node N1.

Now, the reactive power sharing error, denoted as ΔQ_{error} , can be formulated using (8) through (16) in the manner as in (17)-(19):

$$\Delta Q_{error} = \frac{Q_2 - Q_1}{2} \quad (17)$$

$$\Delta Q_{error} = \frac{Q_2 - Q_1}{2} = \frac{X_1 - X_2 - X_{1,2}(1-A)}{2mU_n + X_1 + X_2 + X_{1,2}(1-A)} (Q_1 + Q_2) \quad (18)$$

$$\Delta Q_{error} = \frac{X'_1 - X'_2}{2mU_n + X'_1 + X'_2} (Q_1 + Q_2) \quad (19)$$

As illustrated, equation (19) reveals that the reactive power sharing error is a function of transmission line impedances, the reactive power demand, and the topology of the microgrid. Thus, in pursuit of effective reactive power sharing, there are two potential strategies: i) Increase the transmission line impedances, a course of action that could precipitate significant voltage drops (exceeding 5% of the nominal voltage). This, however, may compromise power system stability; and ii) Opt for a more prudent approach by minimizing the disparities in transmission line impedances. This alternative is characterized by its safety and lack of adverse impact on system stability.

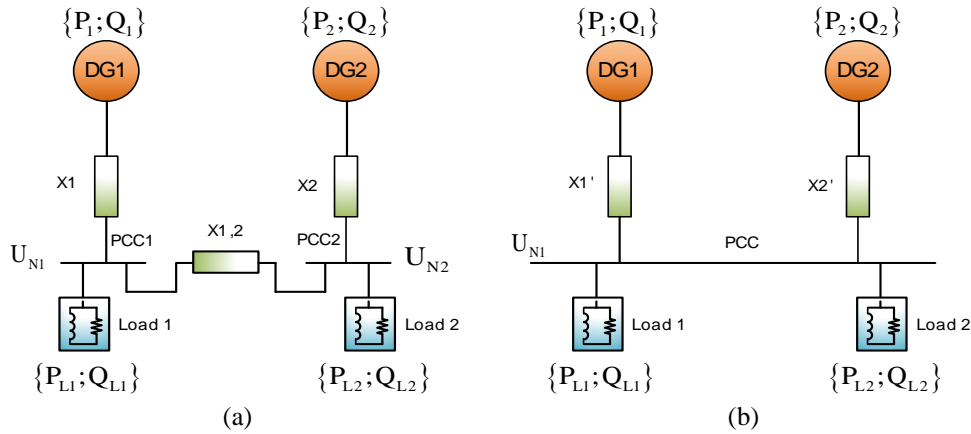


Figure 2. 2 DGs meshed microgrid (a) 2 DGs meshed microgrid equivalent model and (b) simplified form of a 2 DGs meshed microgrid

3. DESIGN OF THE IMPROVED POWER-SHARING METHOD AND SECONDARY CONTROL

3.1. Proposed power sharing method

As previously stated, the traditional control shortcomings are associated mainly with the mismatch of the microgrid's parameters. By compensating this mismatch, the reactive power-sharing issue can be fixed. In this work, we consider a 3 DGs meshed multi-PCC microgrid. The 3 DGs' power ratings are different. 3 Dispersed loads with different power loads are considered. The microgrid consists of 6 buses and the transmission lines are considerably mismatched including the line length. All these mesh operating conditions are considered to test the robustness of the proposed strategy and prove its reliability in the following section. The studied microgrid is inspired by the IEEE 9 bus test feeder as shown in Figure 3.

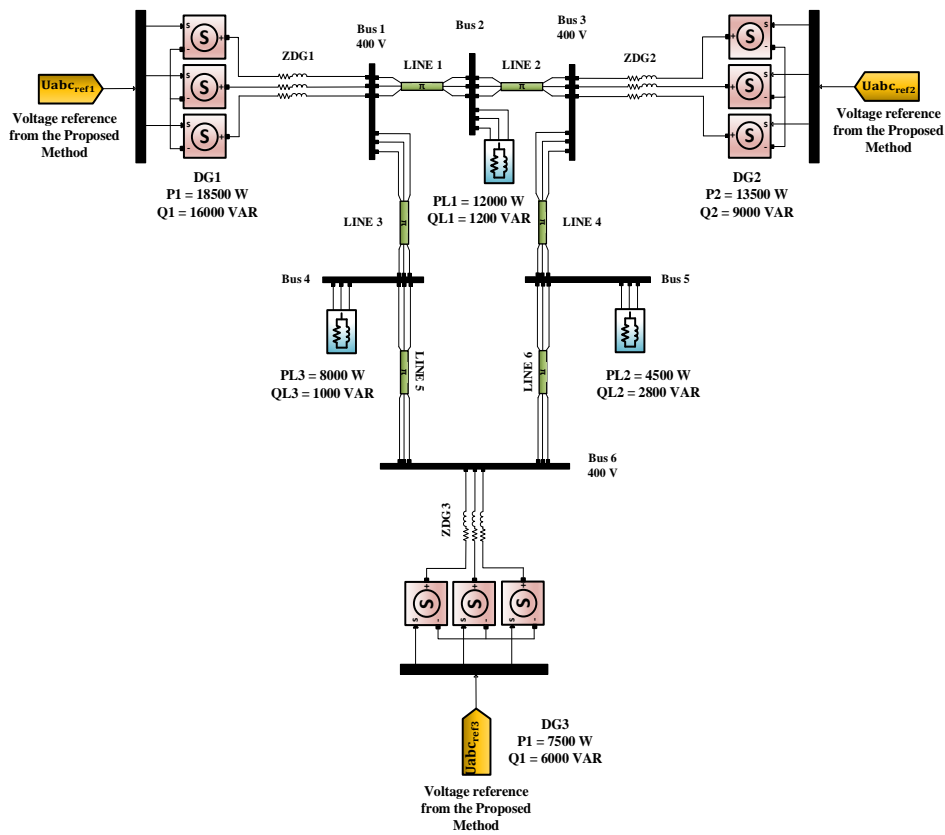


Figure 3. The equivalent model of 2 DGs considered AC meshed microgrid

The parameters of the studied AC microgrid and proposed strategy controllers are specified in Table 1. In this study, the suggested power-sharing scheme is based on the traditional droop control approach. The adopted philosophy consists of preserving the active power equations of the droop control since it is always ensured even under meshed microgrids' structures and operating conditions. As for the Q-V equations, as mentioned earlier, adjusting the output voltage is the key to fixing the reactive power-sharing issues. The suggested control provides two parameters to be corrected: The reactive power and the DGs' output voltage. Suggested method equations are expressed by (20) to (23):

$$w_i = w_{in} - n_i(P_i - P_n) \quad (20)$$

$$U_i = k_i \int (U_n - U_{DG}) dt - k_i \int n_i(Q_i - Q_{in}) dt \quad (21)$$

$$U_{DG} = U_{DG1}, U_{DG2} \text{ or } U_{DG3} \quad (22)$$

$$\text{Where } i = \{1,2,3\} \quad (23)$$

Table 1. Microgrid's setup

Parameter	Value
Rated amplitude U_{in} (phase to phase)	400 V
Nominal frequency f_{in}	50 Hz
Source 1	18,500 W; 16,000 VAR
Source 2	13,500 W; 9,000 VAR
Source 3	7,500 W; 6,000 VAR
Load 1	12,000 W; 1,200 VAR
Load 2	4,500 W; 2,800 VAR
Load 3	8,000 W; 1,000 VAR
DGs' resistor R_{DG}	0.1 Ω
DGs' inductance L_{DG}	1e-3 H
Line impedance L1	0.0690 Ω ; 7.10e-3 H; 50 μ F
Line impedance L2	0.1380 Ω ; 6.4e-3 H; 50 μ F
Line impedance L3	0.207 Ω ; 6.4e-3 H; 50 μ F
Line impedance L4	0.2415 Ω ; 6.1e-3 H; 50 μ F
Line impedance L5	0.1725 Ω ; 6.8e-3 H; 50 μ F
Line impedance L6	0.1035 Ω ; 5e-3 H; 50 μ F

This control aims at the first place to i) Increase the reactive power supplied to each DG to reach its rated value using a PI regulator. This aims to increase the reactive power is translated to a decrease in DGs' output voltage and ii) Voltage regulation: In parallel, a PI regulation is used to keep the DG's output voltage at an acceptable range.

The first PI-Q regulator role is achieving proper reactive power sharing. However, without a voltage regulation, the system stability is lost due to very large voltage deviations. That is why, the two PI regulators are together employed to reach proper power sharing without losing the system stability.

3.2. Secondary control regulation

Typically, even when a primary control system effectively achieves precise active and reactive power sharing, natural frequency and voltage deviations can still arise. Consequently, this paper introduces a secondary control approach. The objective of this secondary control is to assume control after the primary control phase and subsequently restore the network's frequency and voltage to their nominal values, namely 50 Hz and 400 V, respectively. Consequently, corrective terms, δU_i and δw_i , are added to (20) and (21) as it can be seen in (24) to (27):

$$w_i' = w_{in} - n_i(P_i - P_n) + \delta w_i \quad (24)$$

$$U_i = k_i \int (U_n - U_{DG}) - k_i \int n_i(Q_i - Q_{in}) dt + \delta U_i \quad (25)$$

$$\delta w_i = k_f \int (w_n - w_{DG_i}) dt \quad (26)$$

$$\delta U_i = k_U \int (U_n - U_{PCC}) dt \quad (27)$$

k_f and k_U are the proportional integral coefficients for frequency and voltage, respectively.

4. SIMULATION RESULTS AND DISCUSSION

To explore the limitations of droop control in meshed conditions and to address the often-overlooked gaps in the literature, which closely reflect real-world scenarios, multiple simulation scenarios were conducted using MATLAB/Simulink software. In section 4, the simulations are centered around the meshed multi-PCC microgrid depicted in Figure 3, with detailed parameters provided in Table 1. This microgrid configuration serves as the basis for all case studies within this section. Its implementation is carried out within the MATLAB/Simulink software, with each component imported from the software library.

To understand how this simulation is made, Figure 4 illustrates an elaborate schematic diagram outlining the control methodology for an individual DG from Figure 3. The process starts with the measurement of the DG's output voltage, denoted as U_{abci} , and the corresponding current, designated as I_{abci} . These measurements undergo a Park transformation, enabling the calculation of absorbed powers. After this calculation, the active and reactive powers are subjected to filtering. These filtered powers, P_{if} and Q_{if} , serve as inputs to the novel power-sharing controller introduced in this study (20) and (21). A reverse Park Transformation is applied to get at the end the DG_i voltage reference $U_{abci_{ref}}$. Key finding of each simulation scenario is presented in Figure 4.

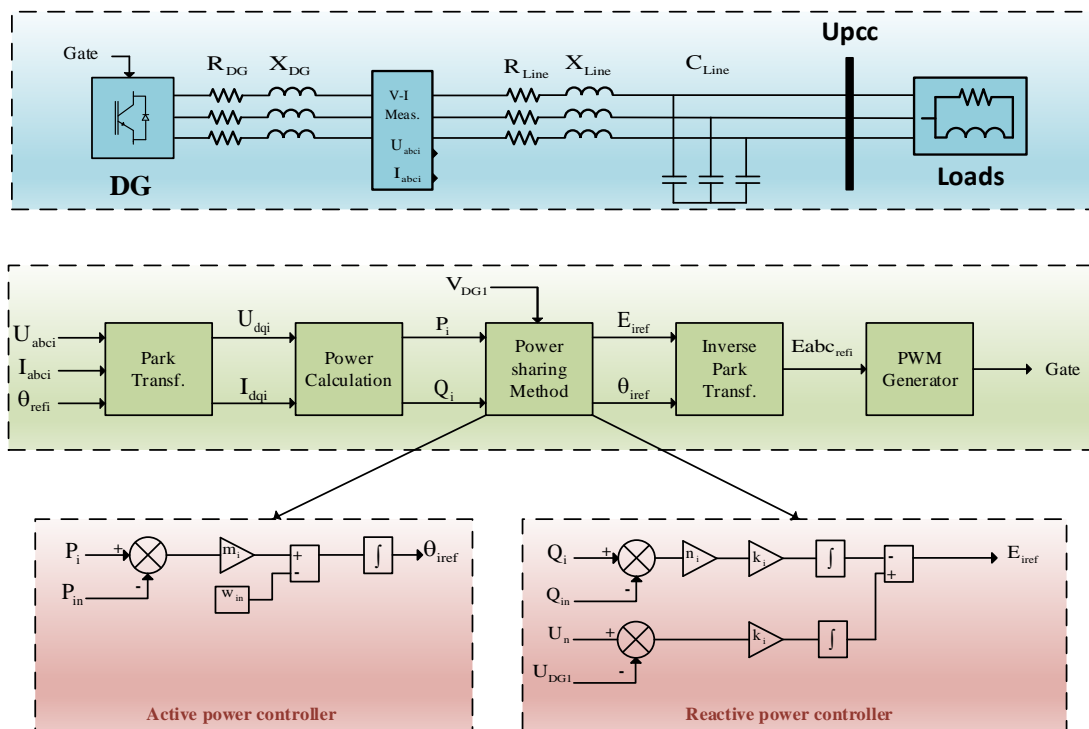


Figure 4. The equivalent model of (2) DGs considered AC meshed microgrid

4.1. Case study 1: conventional droop control

The current case study aims to illustrate the various limitations of the conventional droop control method as outlined in section 3. The microgrid depicted in Figure 3 has been implemented on MATLAB/Simulink relying on (6) and (7). Figure 5 illustrates the performance of the traditional droop control. Throughout the simulation from $t = 0$ s to its conclusion, the three DGs operate simultaneously, while the three loads maintain their operation with a consistent power demand. In Figure 5(a), it is evident that active power sharing is achieved among the three DGs due to the uniform frequency across the microgrid's network, which remains unaffected by parameter modifications. However, in line with expectations, Figure 5(b) highlights the limitation in sharing reactive power through the droop control. Additionally, noticeable deviations in frequency Figure 5(c) and voltage Figure 5(d) are observed. To summarize, these outcomes definitively underscore the fact that the droop control approach struggles to achieve equitable sharing of reactive power within meshed multi-PCC microgrids. Furthermore, substantial frequency and voltage discrepancies may escalate under more challenging operational conditions, such as load fluctuations and alterations in topology. As such, we proved that the droop control method is inefficient for meshed microgrids.

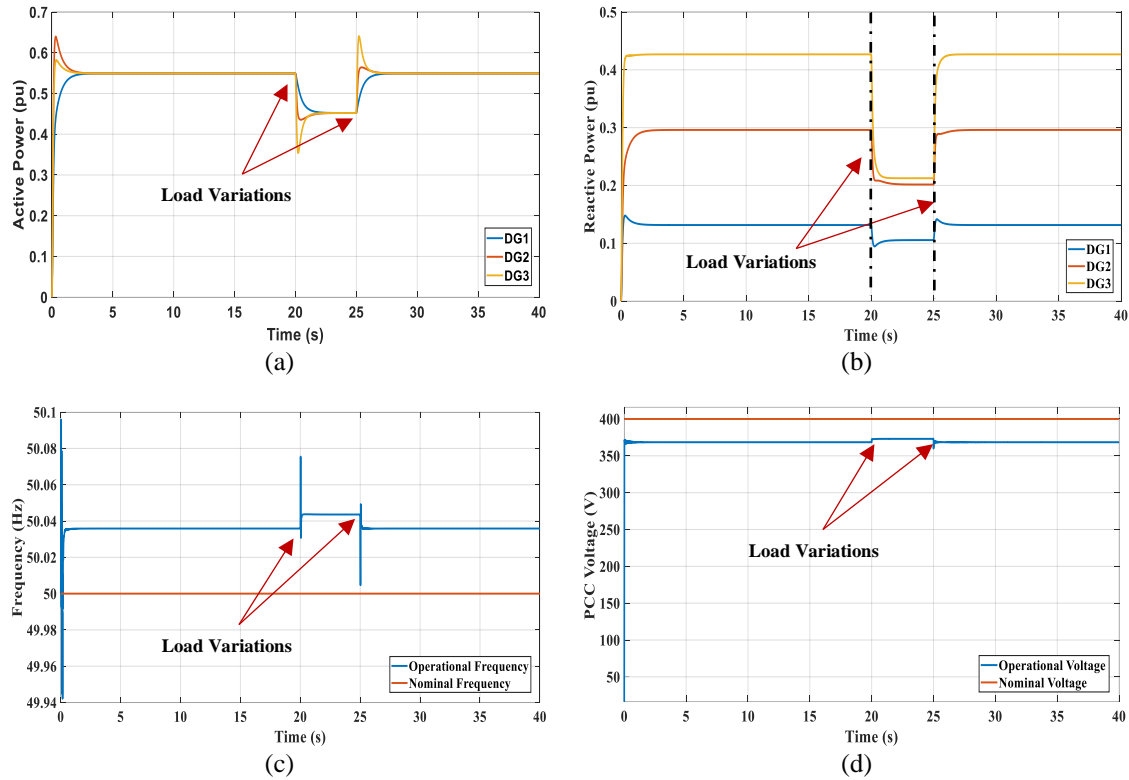


Figure 5. Droop control performances (a) active power, (b) reactive power, (c) frequency, and (d) PCC voltage

4.2. Case study 2: power sharing test of the proposed method

The subsequent case study aims to examine both the conventional droop control and the proposed method to assess the impact of the suggested approach on reactive power. In Figure 6, the time interval from $t = 0$ s to $t = 15$ s employs traditional droop control as the primary mechanism, after which the proposed method takes precedence until the simulation concludes. All three DGs are operational, along with three loads, maintaining a consistent power demand. Figure 6(a) illustrates the equitable distribution of active power during both the droop control and proposed method phases. In Figure 6(b), it is evident that reactive power is not evenly shared during the droop control phase, whereas the suggested method ensures precise sharing of reactive power, even in the presence of significant variations in DG capacities and transmission line impedances. Post $t = 15$ s, the voltage at the PCC exhibits improvement, leading to an increase in P_i at $t = 15$ s. However, notable deviations in frequency and voltage persist, as secondary control measures have not yet been introduced, as depicted in Figures 6(c) and (d). In summary, we proved that the proposed method ensures precise power sharing, even in the presence of significant variations in distributed generators' capacities and transmission line impedances, aspects often overlooked in the existing literature.

4.3. Case study 3: robustness test of the proposed method

The primary objective of this particular case study is to assess the resilience and reliability of the suggested method. Specifically, the study takes into account variations in load and changes in the system's topology. In Figure 7, the time interval from $t = 0$ s to $t = 15$ s employs traditional droop control, and from $t = 15$ s until the simulation's conclusion, the suggested method is implemented. Throughout this period, all three DGs are in operation. Noteworthy events occur within the simulation timeline: at $t = 20$ s, load 2 is deactivated, and at $t = 25$ s, it is subsequently reconnected. Additionally, line 3 undergoes disconnection and reconnection at $t = 30$ s and $t = 35$ s, respectively.

Figures 7(a) and (b) illustrate that the accuracy of power-sharing remains unaffected by the changes in loads and alterations to the system's topology. This consistent performance under varying conditions validates the robustness of the proposed method. It is important to note that the inclusion of secondary control measures has not yet been realized, resulting in notable frequency and voltage deviations, as evidenced in Figures 7(c) and (d). In summary, we proved that the proposed method keeps precise power sharing, even in the presence of meshed scenarios, aspects often overlooked in the existing literature.

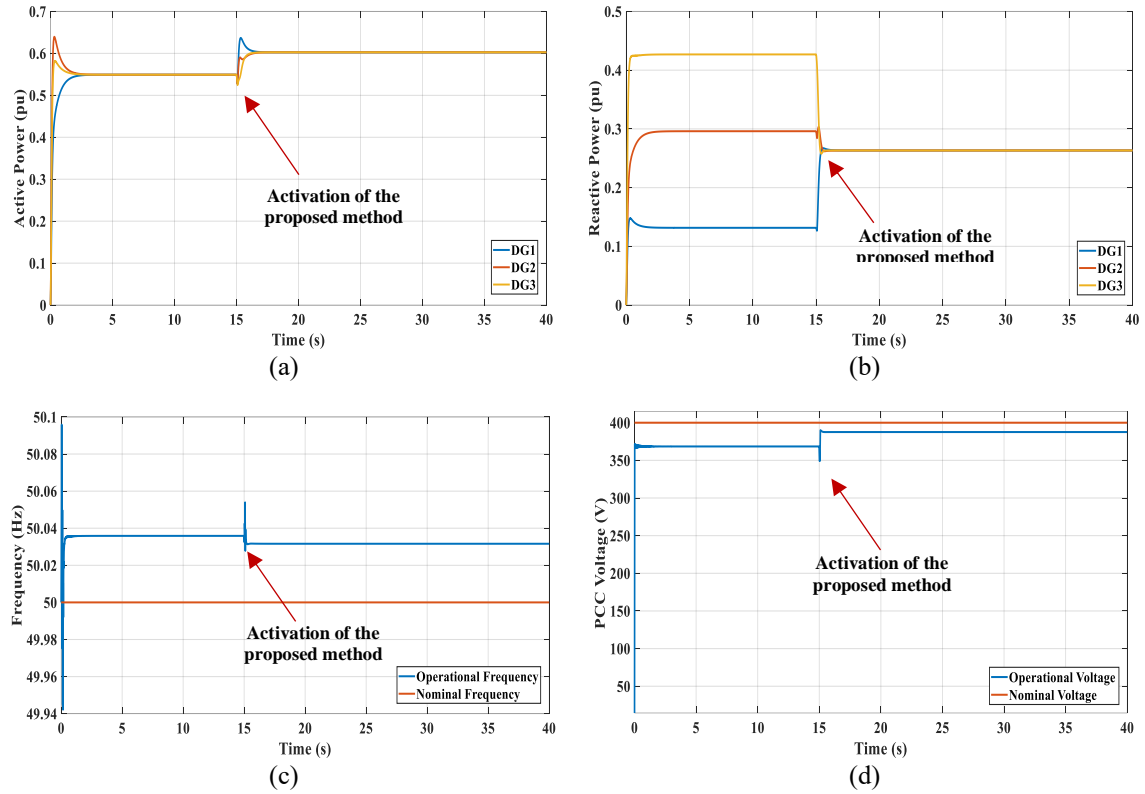


Figure 6. Power sharing method performances: (a) active power, (b) reactive power, (c) frequency, and (d) PCC voltage

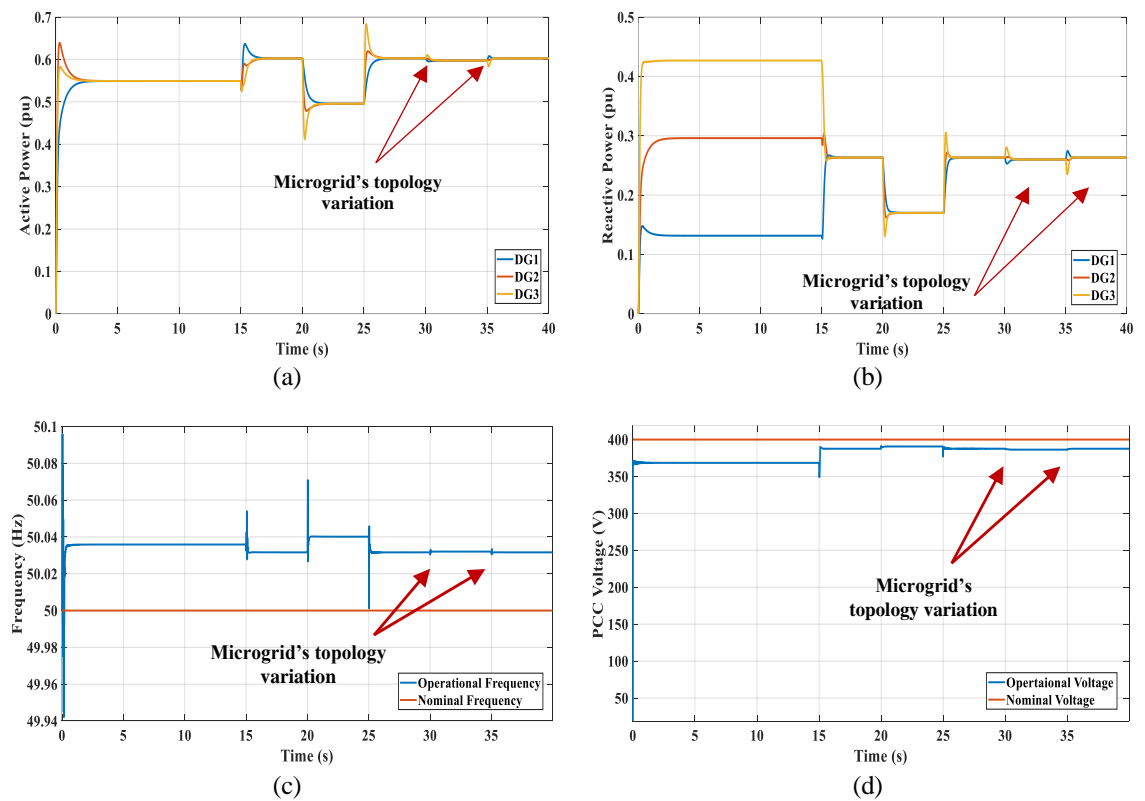


Figure 7. Robustness test of the proposed method (a) active power, (b) reactive power, (c) frequency, and (d) PCC voltage

4.4. Case study 4: secondary control test of the proposed method

The primary objective of this particular case study is to rectify the frequency and voltage deviations introduced by the initial control mechanism. As depicted in Figure 8, the period from $t = 0$ s to $t = 15$ s employs droop control, after which the suggested method takes precedence until the simulation concludes. Notably, load variations and changes in the system's configuration are taken into account.

In Figure 8, the activation of secondary control occurs at $t = 18$ s. Before the activation of secondary control, significant frequency and voltage deviations are evident, as shown in Figures 8(a) and (b), respectively. However, following $t = 18$ s, the operational frequency and point of common coupling (PCC) voltage closely align with their nominal values. Furthermore, as observed in Figures 8(c) and (d), the introduction of secondary control did not compromise the accuracy of power sharing among the DGs. In summary, our approach demonstrates that power sharing and secondary control performances remain unaffected by all the meshed conditions examined in this paper. Conversely, existing methods in the literature overlook meshed conditions in their analysis, potentially leading to instabilities as they are not designed for such scenarios.

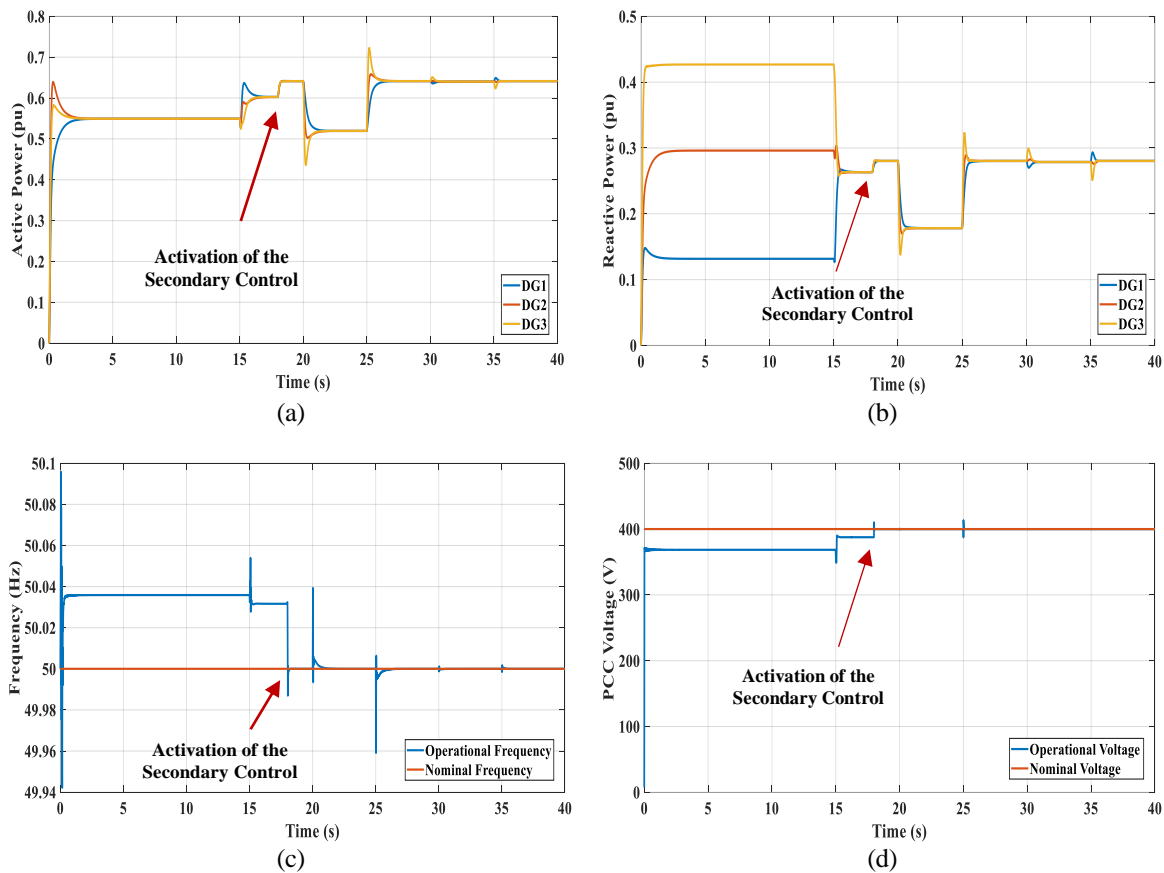


Figure 8. Secondary control performances (a) active power, (b) reactive power, (c) frequency, and (d) PCC voltage

5. EXPERIMENTAL VALIDATION

The proposed power sharing and secondary controllers were implemented and validated in real-time using a hardware-in-loop (HIL) simulator, as depicted in Figure 9. The control logic was executed on the PXIe-1082 board, which generated gating signals. For consistency, we utilized the same microgrid configuration as studied in the simulations section, implemented in MATLAB/Simulink software.

In HIL simulations, a real-time model mirroring the physical characteristics of the microgrid was generated based on the microgrid presented in Figure 3 and its parameters in Table 1. The control systems of this model were constructed based on (24) and (25) to integrate primary and secondary controls into the power system model. This model was seamlessly integrated into the National Instruments PXIe-1072 system through the Opal-RT interface. The PXIe-1072 system facilitated the delivery of digital inputs for gating signals to the

DGs inverters and the transmission of analog outputs for feedback signals to the control system. The entire control framework was developed within the dSPACE environment using the MicroLabBox system, as illustrated in Figure 9.



Figure 9. Photograph of the experimental setup

5.1. Experimentation 1: power sharing

In Figures 10(a) and (b), the time interval spanning from $t = 0$ s to $t = 20$ s illustrates the utilization of droop control. Subsequently, after $t = 20$ s, the proposed method assumes control. During the droop control phase (0 to 20 s), the distribution of active power is accomplished, whereas, as expected, reactive power sharing is not realized. In contrast, during the proposed method phase (20 s to the conclusion of the simulation), active power sharing is always ensured, and precise sharing of reactive power is successfully achieved as well. Additionally, the experimental outcomes closely correspond to the simulation results presented in Figures 6(a) and (b).

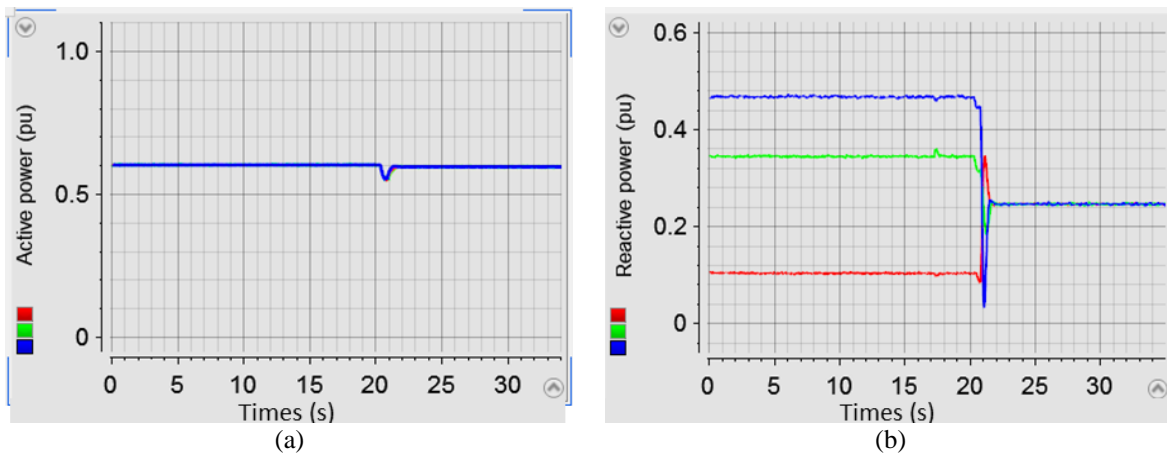


Figure 10. Experimental results for the power-sharing test (a) active power sharing test and (b) reactive power sharing test

5.2. Experimentation 2: power sharing robustness

In Figures 11(a) and (b), the time interval spanning from $t = 0$ s to $t = 20$ s illustrates the application of droop control. Subsequently, after $t = 20$ s, the proposed method takes charge. Noteworthy events occur within the simulation timeline: load 2 undergoes disconnection and reconnection at $t = 40$ s and $t = 60$ s, respectively, while line 3 experiences disconnection and reconnection at $t = 80$ s and $t = 100$ s, respectively. Notably, the robustness test conducted has demonstrated that power-sharing accuracy remains unaffected. Moreover, the experimental findings closely mirror the simulation outcomes presented in Figures 7(a) and (b).

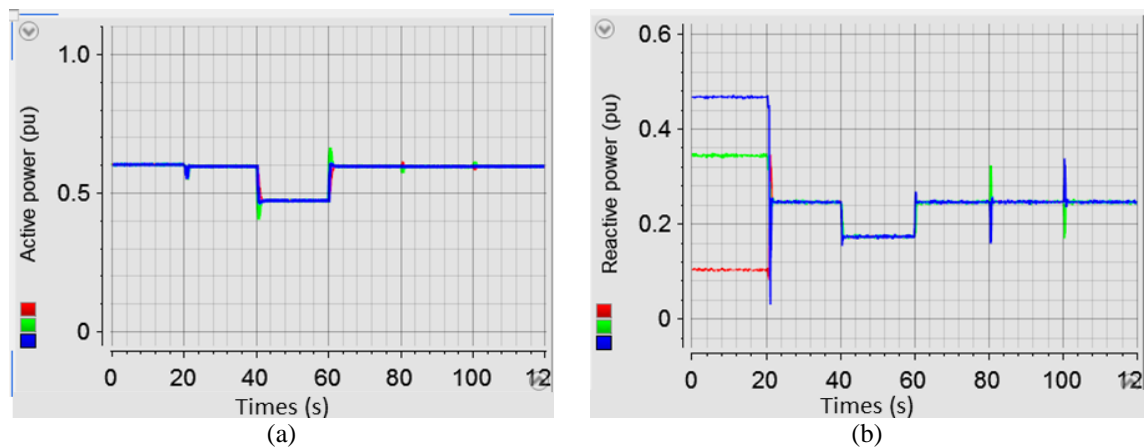


Figure 11. Experimental results for the robustness test (a) active power robustness test and (b) reactive power robustness test

6. CONCLUSION

This paper introduces a straightforward and resilient power-sharing technique adopted for islanded AC meshed multi-PCC microgrids. Through theoretical analysis, it was established that achieving proper sharing of reactive power among parallel DGs is hindered by the mismatched impedances of feeders and the complex meshed microgrid configurations. Consequently, the proposed methodology aims to address these challenges within a meshed multi-PCC microgrid involving three DGs, considering different power ratings, load fluctuations, and alterations in microgrid topology. Incorporating these intricate constraints, the proposed method ensures accurate sharing of both active and reactive power. Nonetheless, noticeable deviations in frequency and voltage from their nominal values were observed. A secondary control strategy is introduced to address this concern. As a result, the secondary control effectively restores frequency and voltage to their desired levels, while simultaneously preserving the accuracy of power distribution. The efficiency of the proposed control strategies is validated through diverse scenarios, employing both the MATLAB/Simulink platform and the HIL simulator. The obtained results affirm the effectiveness and resilience of both the primary and secondary controls. Looking ahead, the future trajectory involves delving into a stability analysis of this method.




REFERENCES

- [1] M. Beuse, B. Steffen, M. Dirksmeier, and T. S. Schmidt, "Comparing CO2 emissions impacts of electricity storage across applications and energy systems," *Joule*, vol. 5, no. 6, pp. 1501–1520, Jun. 2021, doi: 10.1016/j.joule.2021.04.010.
- [2] A. Papageorgiou, A. Ashok, T. Hashemi Farzad, and C. Sundberg, "Climate change impact of integrating a solar microgrid system into the Swedish electricity grid," *Applied Energy*, vol. 268, Jun. 2020, doi: 10.1016/j.apenergy.2020.114981.
- [3] A. Jäger-Waldau, "Snapshot of Photovoltaics—February 2019," *Energies*, vol. 12, no. 5, Feb. 2019, doi: 10.3390/en12050769.
- [4] N. T. Hai and K.-H. Kim, "An adaptive virtual impedance based droop control scheme for parallel inverter operation in low voltage microgrid," *International Journal of Power Electronics and Drive Systems*, vol. 7, no. 4, pp. 1309–1319, Dec. 2016, doi: 10.11591/ijpeds.v7.i4.pp1309-1319.
- [5] Y. Gupta, N. Parganiha, A. K. Rathore, and S. Doolla, "An improved reactive power sharing method for an islanded microgrid," *IEEE Transactions on Industry Applications*, vol. 57, no. 3, pp. 2954–2963, May 2021, doi: 10.1109/TIA.2021.3064528.
- [6] Z. Jin, X. Wang, F. Liu, K. Xin, and Y. Liu, "A voltage-droop-free reactive power sharing solution in microgrids," in *2020 IEEE 9th International Power Electronics and Motion Control Conference (IPEMC2020-ECCE Asia)*, IEEE, Nov. 2020, pp. 3323–3328. doi: 10.1109/IPEMC-ECCEAsia48364.2020.9367665.
- [7] N. Ghanbari and S. Bhattacharya, "Adaptive droop control method for suppressing circulating currents in DC microgrids," *IEEE Open Access Journal of Power and Energy*, vol. 7, pp. 100–110, 2020, doi: 10.1109/OAJPE.2020.2974940.




- [8] T. Nguyen, H. Nguyen, Y. Wang, O. Mohammed, and E. Anagnostou, "Distributed secondary control in microgrids using synchronous condenser for voltage and frequency support," *Energies*, vol. 15, no. 8, Apr. 2022, doi: 10.3390/en15082968.
- [9] Y. Hennane, Y. A. Ait Ben Hassi, A. Berdai, and V. Tytiuk, "Primary, secondary and tertiary controls of a mesh multi-PCC microgrid," in *2022 IEEE 4th International Conference on Modern Electrical and Energy System (MEES)*, IEEE, Oct. 2022, pp. 1–5, doi: 10.1109/MEES58014.2022.10005647.
- [10] M. Savaghebi, A. Jalilian, J. C. Vasquez, and J. M. Guerrero, "Secondary control for voltage quality enhancement in microgrids," *IEEE Transactions on Smart Grid*, vol. 3, no. 4, pp. 1893–1902, Dec. 2012, doi: 10.1109/TSG.2012.2205281.
- [11] Q. Shafiee, J. M. Guerrero, and J. C. Vasquez, "Distributed secondary control for islanded microgrids—a novel approach," *IEEE Transactions on Power Electronics*, vol. 29, no. 2, pp. 1018–1031, Feb. 2014, doi: 10.1109/TPEL.2013.2259506.
- [12] Y. A. Ait Ben Hassi, Y. Hennane, A. Berdai, and V. Tytiuk, "A robust reactive power sharing solution for meshed multi-PCC microgrids," in *2023 17th International Conference on Engineering of Modern Electric Systems (EMES)*, IEEE, Jun. 2023, pp. 1–4, doi: 10.1109/EMES58375.2023.10171691.
- [13] Y. A. Ait Ben Hassi, Y. Hennane, A. Berdai, and V. Tytiuk, "Primary and secondary controls with reactive power sharing in mesh microgrids," in *2022 IEEE 4th International Conference on Modern Electrical and Energy System (MEES)*, IEEE, Oct. 2022, pp. 1–6, doi: 10.1109/MEES58014.2022.10005740.
- [14] L. Jia, C. Du, C. Zhang, and A. Chen, "An improved droop control method for reducing current sensors in DC microgrid," in *2017 Chinese Automation Congress (CAC)*, IEEE, Oct. 2017, pp. 4645–4649, doi: 10.1109/CAC.2017.8243599.
- [15] Y. Han, X. Ning, L. Li, P. Yang, and F. Blaabjerg, "Droop coefficient correction control for power sharing and voltage restoration in hierarchical controlled DC microgrids," *International Journal of Electrical Power and Energy Systems*, vol. 133, Dec. 2021, doi: 10.1016/j.ijepes.2021.107277.
- [16] M. I. Azim *et al.*, "A proportional power sharing method through a local control for a low-voltage islanded microgrid," *Energy Reports*, vol. 8, pp. 51–59, Dec. 2022, doi: 10.1016/j.egy.2022.10.119.
- [17] H. Shadabi and I. Kamwa, "Dual Adaptive Nonlinear droop control of VSC-MTDC system for improved transient stability and provision of primary frequency support," *IEEE Access*, vol. 9, pp. 76806–76815, 2021, doi: 10.1109/ACCESS.2021.3078066.
- [18] H. Sellamna, A. M. Pavan, A. Mellit, and J. M. Guerrero, "An iterative adaptive virtual impedance loop for reactive power sharing in islanded meshed microgrids," *Sustainable Energy, Grids and Networks*, vol. 24, Dec. 2020, doi: 10.1016/j.segan.2020.100395.
- [19] X. H. T. Pham, "An improved controller for reactive power sharing in islanded microgrid," *Electrical Engineering*, vol. 103, no. 3, pp. 1679–1689, Jun. 2021, doi: 10.1007/s00202-020-01160-x.
- [20] K. O. Oureilidis and C. S. Demoulias, "A decentralized impedance-based adaptive droop method for power loss reduction in a converter-dominated islanded microgrid," *Sustainable Energy, Grids and Networks*, vol. 5, pp. 39–49, Mar. 2016, doi: 10.1016/j.segan.2015.11.003.
- [21] J. He and Y. W. Li, "An enhanced microgrid load demand sharing strategy," *IEEE Transactions on Power Electronics*, vol. 27, no. 9, pp. 3984–3995, Sep. 2012, doi: 10.1109/TPEL.2012.2190099.
- [22] Y. Hu, J. Xiang, Y. Peng, P. Yang, and W. Wei, "Decentralised control for reactive power sharing using adaptive virtual impedance," *IET Generation, Transmission and Distribution*, vol. 12, no. 5, pp. 1198–1205, Mar. 2018, doi: 10.1049/iet-gtd.2017.1036.
- [23] Y. Zhu, F. Zhuo, F. Wang, B. Liu, and Y. Zhao, "A wireless load sharing strategy for islanded microgrid based on feeder current sensing," *IEEE Transactions on Power Electronics*, vol. 30, no. 12, pp. 6706–6719, Dec. 2015, doi: 10.1109/TPEL.2014.2386851.
- [24] A. Micallef, M. Apap, C. Spiteri-Staines, J. M. Guerrero, and J. C. Vasquez, "Reactive power sharing and voltage harmonic distortion compensation of droop controlled single phase islanded microgrids," *IEEE Transactions on Smart Grid*, vol. 5, no. 3, pp. 1149–1158, May 2014, doi: 10.1109/TSG.2013.2291912.
- [25] J. W. Simpson-Porco, Q. Shafiee, F. Dorfler, J. C. Vasquez, J. M. Guerrero, and F. Bullo, "Secondary frequency and voltage control of islanded microgrids via distributed averaging," *IEEE Transactions on Industrial Electronics*, vol. 62, no. 11, pp. 7025–7038, Nov. 2015, doi: 10.1109/TIE.2015.2436879.
- [26] H. Han, Y. Liu, Y. Sun, M. Su, and J. M. Guerrero, "An Improved droop control strategy for reactive power sharing in islanded microgrid," *IEEE Transactions on Power Electronics*, vol. 30, no. 6, pp. 3133–3141, Jun. 2015, doi: 10.1109/TPEL.2014.2332181.
- [27] C. Dou, M. Lv, T. Zhao, Y. Ji, and H. Li, "Decentralised coordinated control of microgrid based on multi-agent system," *IET Generation, Transmission and Distribution*, vol. 9, no. 16, pp. 2474–2484, Dec. 2015, doi: 10.1049/iet-gtd.2015.0397.
- [28] J. Schiffer, T. Seel, J. Raisch, and T. Sezi, "Voltage stability and reactive power sharing in inverter-based microgrids with consensus-based distributed voltage control," *IEEE Transactions on Control Systems Technology*, vol. 24, no. 1, pp. 96–109, Jan. 2016, doi: 10.1109/TCST.2015.2420622.
- [29] Y. Hennane, A. Berdai, J.-P. Martin, S. Pierfederici, and F. Meibody-Tabar, "New decentralized control of mesh AC microgrids: study, stability, and robustness analysis," *Sustainability*, vol. 13, no. 4, Feb. 2021, doi: 10.3390/su13042243.
- [30] Y. Hennane, J.-P. Martin, A. Berdai, S. Pierfederici, and F. Meibody-Tabar, "Power sharing and synchronization strategies for multiple PCC islanded microgrids," *International Journal of Electrical and Electronic Engineering and Telecommunications*, pp. 156–162, 2020, doi: 10.18178/ijeetc.9.3.156-162.

BIOGRAPHIES OF AUTHORS






Youssef Amine Ait Ben Hassi    received the engineering degree in electrical engineering from Ecole Nationale Supérieure d'Electricité et de Mécanique (ENSEM), Casablanca, Morocco, in 2020. In pursuit of his academic aspirations, he subsequently joined the Ph.D. program in electrical engineering at the Energy and Electrical Systems Laboratory (LESE) of Hassan II University in Casablanca. His research interests primarily focus on the development of innovative approaches for controlling microgrids and power systems. He also actively contributes to the field of their modeling, aiming to enhance the understanding and optimization of microgrid and power system dynamics. He can be contacted at email: youssefamine.aitbenhassi@gmail.com.



Youssef Hennane    attained in 2015 his Engineering degree in electrical engineering from Ecole Normale supérieure de l'Enseignement Technique (ENSET), located in Mohammadia, Morocco. He further pursued a collaborative Ph.D. program in electrical engineering, completing it at CNRS, LEMTA, Université de Lorraine in Nancy, France, and the LESE Laboratory, Hassan II University. His research focuses on the intricate domains of power systems and microgrids, including the effective management and optimization of electrical networks in the context of distributed generation systems. He can be contacted at email: youssefhennane@gmail.com.



Abdelmajid Berdai    completed his Ph.D. in engineering and has since held the position of professor and Department Chair of Electrical Engineering at the National School of Electricity and Mechanics (ENSEM), within Hassan II University, Casablanca, Morocco, starting in 1996. Since 2002, he has actively contributed to the Laboratory Building Technologies and Industrial Systems (TCSI), as part of the Research Group: Electrical Systems (ESE). Notably, he has contributed significantly to academia through his numerous publications in reputable journals and conferences. Berdai's research pursuits encompass the dynamic simulation of electric machinery, as well as the simulation and optimization of renewable energy systems. His work also delves into the application of quality power conversion for monitoring the state of electromechanical equipment, alongside the estimation of modes and diagnosis of induction motors based on the quality of energy conversion. Additionally, he has served as a reviewer for the Elsevier Journal and has taken on significant roles such as session chair, TPC chair, and panelist in various conferences. He can be contacted at email: a.berdai@gmail.com.